A COMPARISON OF HUMAN AND IDEAL PERFORMANCE FOR THE DETECTION OF VISUAL PATTERN

A THESIS
SUBMITTED TO THE FACULTY OF THE GRADUATE SCHOOL
OF THE UNIVERSITY OF MINNESOTA

BY

DANIEL JOHN KERSTEN

IN PARTIAL FULFILLMENT OF THE REQUIREMENTS
FOR THE DEGREE OF
DOCTOR OF PHILOSOPHY
June, 1983

Chapter 3: Spatial-Frequency Summation in Visual Noise

Abstract. Contrast thresholds were measured for sinusoidal gratings of frequencies 2 and 6 c/deg and for compound gratings consisting of the superposition of these two gratings. The gratings were enveloped by a Gaussian of width equal to .5° between 1/e points. Thresholds were compared for three conditions: (1) in the presence or absence of dynamic visual noise, (2) in peaks-add or peaks-subtract phase and (3) with signal certainty or uncertainty. Psychometric functions were also measured for the 2 and 6 c/deg gratings in the presence and absence of noise.

Spatial-frequency summation in visual noise is similar to summation in the absence of noise, although the psychometric function slopes are shallower in noise. There was no significant effect of relative phase on the amount of summation. For the third condition, there was less summation when the observer was given prior information concerning which stimulus was to be presented.

Several models of summation are considered. It is suggested that the results are approximated by "ideal summation". This means that after allowing for the difference in relative sensitivity for the two gratings, detection is based on the contrast energy of the compound grating.

INTRODUCTION

A central problem in visual perception is the prediction of threshold for an arbitrary pattern. An important related problem is to understand how physiological mechanisms might explain detection. One approach to these problems has been to try to understand how the detectability of small spots of light relates to the detectability of more complicated targets such as a combination of several spots (cf. Blackwell, 1963; Cohn and Lasley, 1975).

A second approach, often referred to as "systems analysis", describes the visual response by the convolution of the image with the "response function" of the visual system. These models, also called "single-channel" models, have used both spatial frequency and spatial descriptions of the stimuli (cf. Schade, 1956; Kelly, 1961; Ratliff, 1965).[1]

A third approach is the extension of the single-channel approach to the spatial frequency analysis of contrast detection in terms of several spatial frequency channels. This third, or multiple-channels approach was initiated when Campbell and Robson (1968) suggested that pattern detection was mediated by independent spatial frequency selective mechanisms. This conjecture was based on the observation that medium to high spatial frequency square waves became visible when the fundamental reached its own independent threshold. One paradigm, used to investigate single- vs. multiple-channel models of

detection, has been to compare thresholds for two-component gratings with thresholds found for individual components. These studies are referred to as grating summation or spatial-frequency summation experiments. The results of these and related sub-threshold summation experiments have been used to devise models of detection (Limb and Rubenstein, 1977; Graham, Robson and Nachmias, 1978; Quick, Mullins and Reichert, 1978; Legge, 1978; Wilson and Bergen, 1978; Watson, 1982).

The spatial-frequency summation paradigm is used in this chapter to explore the applicablity of single- and multiple-channel models to detection of patterns consisting of one or two sinusoidal gratings embedded in dynamic visual noise. Visual noise provides a rigorous way to investigate high contrast detection by raising contrast

---

[1]Because confusion often arises over the meaning of "channel", it will be defined for the purposes of this study as follows. A channel is a linear mechanism which takes as input the luminance function of a stimulus (which may be one or two spatial dimensions and may or may not include time) and produces a filtered image (cf. Graham, 1980, p. 218). The filtering operation is typically represented in the space domain by a convolution, or in the spatial frequency domain by multiplication by a modulation transfer function. In the latter case, a channel is called a "spatial-frequency channel". Physiological representations are often ascribed to these channels, the components of which are neurons which have similar receptive field properties. The output of a channel is then thought of as a "neural image" (cf. Robson, 1980).

thresholds. Comparison is made with results obtained in the absence of noise under otherwise identical conditions.

Review of two-component grating research

The detectability of patterns consisting of two superposed gratings was first studied by Graham and Nachmias (1971), although analogous problems in audition had been studied much earlier (Green, 1958). Graham and Nachmias tested the hypotheses of single- vs. multiple-channel models of pattern detection using combinations of gratings of frequencies f and 3f. (Such combinations will be referred to as compound gratings, as distinct from single component gratings referred to as simple gratings.) They used two phase relations. In the peaks-add form, the peaks of the f and 3f components were spatially coincident. In the peaks-subtract form, the peak of the f component was coincident with the trough of the 3f component. Contrast thresholds were found to be independent of the relative phase relation between the two components in the compound grating. The detectability of the pattern composed of two sinusoidal components was limited almost solely by the detectability of its most detectable component. That is, there was little or no spatial-frequency summation. (Summation is said to occur when the detectability of one of the components of a compound grating is greater than when presented alone.) They interpreted their results as support for a multiple-channels model of visual detection.

In the same year, Sachs, Nachmias and Robson (1971) reported measurements of psychometric functions for simple and compound gratings with f=14 c/deg. They found evidence of the independent detection of the components f and f' for compound gratings as long as f' was at least 25% greater or less than f. Independent detection was taken to mean that the small summation observed was consistent with probability summation. The difference found between psychometric function shapes was consistent with a multiple-channels model in which the spatial frequency channels are less than an octave wide.

Pantle (1973) found that f plus 2f combinations showed increasing summation as the spatial frequency (f) was lowered from 5 to 1 c/deg for slowly drifting gratings (.03 Hz of the f component). Summation also increased as the gratings were drifted from 0 to 8 Hz with respect to the f component. He suggested that spatial frequency tuning curves broaden as drift rate increases. The finding of increased summation for the lower spatial frequency suggests broader tuning curves (on logarithmic coordinates) for lower spatial frequencies.

Quick and Reichert (1975) found that the degree of summation as a function of f'-f on a linear scale was invariant for spatial frequencies of 7.4, 14.8 and 21 c/deg. They interpreted this finding as evidence of channels representing a fixed area of the visual field

rather than as consisting of a constant number of cycles. That is, on logarithmic coordinates, the tuning curves of the hypothesized spatial frequency channels become narrower as the center frequency increases.

Mostafavi and Sakrison (1976) measured contrast thresholds for combinations of static isotropic narrow-band noise components with center frequencies 4.5 and 6 c/deg and also for combinations of 4.5 and 18 c/deg. They found evidence for the independent detection of each component for the 4.5 and 18 c/deg combination, but not for the 4.5 plus 6 c/deg combination.

Limb and Rubinstein (1977) measured contrast thresholds for 3.3 and 9.9 c/deg gratings. The width (2.7^{o}) corresponded to about 9 cycles of the 3.3 c/deg grating. Viewing was 500' peripheral to the fovea. They found less summation for the peaks-add combination than the peaks-subtract combination. They also report that more summation was found for the narrowly windowed gratings than for broader windows (11^{o}), although no data was shown for the latter case. They proposed a single-channel model which took into account spatial inhomogeneities of the visual system. Assuming homogeneity in a region 2.7^{o} led to a prediction of more summation than was found.

Quick, Mullins and Reichert (1978) pointed out that if probability summation across space is included in calculations of bandwidth based on spatial-frequency summation data, the calculated

bandwidths are wider than without spatial summation. They calculated bandwidths of 6 c/deg corresponding to fundamental component frequencies of 11.8, 14.8 and 21 c/deg and a bandwidth of 3 c/deg for a 5 c/deg component.

Graham, Robson and Nachmias (1978) measured grating summation in the fovea and periphery. They controlled for signal-uncertainty by randomly interleaving the stimuli. The gratings were well localized in space and spatial frequency and in time and temporal frequency with Gaussian windows. Also, in distinction with the above studies, they used a two-alternative forced-choice procedure. Using Quick's (1974) form of the psychometric function, they accounted for their results in terms of probability summation among several detectors at each retinal location. In particular, this model predicts the amount of grating summation from the psychometric function slope. They also suggested that there should be less summation when the stimuli are not interleaved because this would lower the thresholds of the simple gratings but not the compound ones. This is because the observer is assumed to be able to attend to spatial frequency filters tuned to the simple gratings when the stimuli are not interleaved. According to their model, there are no filters matching the compound grating. That is, the observer is intrinsically uncertain for compound gratings.

Bergen, Wilson and Cowan (1979) measured subthreshold summation

for sinusoidal gratings, difference of Gaussians (DOGs) and square waves. They accounted for their summation data with the four-mechanism model of Wilson and Bergen (1979). This model incorporates spatial summation and summation over four classes of detectors with bandwidths at half-height of 1.75 octaves. Watson (1982), however, required at least 7 classes of frequency- selective detectors of narrower bandwidth (about 1 octave) to account for his two-component grating summation data.

There have been at least two studies which have tried to extend the subthreshold summation paradigm described above to suprathreshold levels. Quick, Hamerly and Reichert (1976) had observers match the apparent contrast of two-component compound gratings (4 and 12 c/deg, and 4 and 20 c/deg) to a 6.25 c/deg test grating of fixed contrast. For contrasts below 20%, apparent contrast was determined by the r.m.s. contrast. They also had observers make contrast matches to stationary one-dimensional noise patterns. After allowing for variation in sensitivity with spatial frequency, r.m.s. contrast matches were approximately constant as a function of bandwidth from about 1 to 20 c/deg.

In contrast to the findings of Quick, Hamerly and Reichert (1976), Arend and Lange (1980) using a similar paradigm, found that apparent contrast of a compound grating (5 and 15 c/deg) was dominantly determined by the apparent contrast of the component with

the higher apparent contrast. Their derived spatial-frequency bandwidths at high contrasts were relatively narrow and were about the same as those derived from threshold measurements. Both of the above studies found no effect of peaks-add vs. peaks-subtract relative phases for spatial frequencies sufficiently separated.

To summarize, the detectability of a two-component grating is only slightly greater than that of its most detectable component. An analogous result may hold for contrast matching experiments using the two-component grating paradigm. A popular explanation for the small summation found is in terms of probability summation. However, the above review has raised several questions which will be addressed here.

Questions concerning spatial-frequency summation

1) How is summation affected by noise level?

Increasing noise level raises contrast thresholds. Thus the study of detection in noise provides another way of investigating otherwise suprathreshold levels. This technique might provide insight to the findings of Quick, Hamerly and Reichert (1976) and Arend and Lange (1980) reviewed above. It has been shown that efficiency for detection in noise remains high for gratings windowed as narrowly as an eighth of a cycle (Chapter 2). This suggests that information across a wide range of spatial frequencies is combined very efficiently. In the present study, the grating of the lower

frequency component (2 c/deg) was confined to one cycle between 1/e points of a Gaussian envelope. This corresponds to 2.2 octaves as measured between the 1/e points of the spatial frequency spectrum (which is a Gaussian). Previous measurements suggested that this width leads to highest detection efficiency for a 2 c/deg grating in noise.

2) Is summation under the conditions of these experiments "ideal summation"?

The performance of the ideal observer for the signal-certain spatial-frequency summation task (described below) is uniquely determined by the contrast energy of the pattern, for a fixed noise level (see RESULTS and DISCUSSION). The human observer shows differences in sensitivity for various spatial frequencies, which of course is not the case for the ideal. Suppose differences in sensitivity, are allowed for by normalizing contrast by the contrast threshold. Then we can ask whether the threshold for compound gratings is determined by its normalized contrast energy. The summation found for patterns in the absence of noise is typically less than predicted by ideal summation (see RESULTS and DISCUSSION). It is not clear whether this is always true, or whether it is true for gratings in noise.

3) Is there an effect of stimulus uncertainty on:

a) contrast thresholds?

b) summation?

As mentioned above, Graham, Robson and Nachmias (1978) suggested that there might be more summation when the observer does not know which signal will appear in a given trial. They found that the proportion correct for the detection of randomly interleaved, as compared with non-interleaved gratings, did not change significantly for 3 and 9 c/deg combinations, but was significantly less for the individual components. If we assume that $\underline{d}' \propto \underline{c}^3$, the maximum change in contrast threshold predicted from their results is only 18%. The predicted effect of uncertainty on contrast threshold based on ideals is also small. Pelli (1981) shows signal-to-noise ratio thresholds for ideal observers which are uncertain for between 1 and 10,000 possible signals (see his bottom panel, Fig. 5.4, following page 140). The predicted difference in contrast threshold between ideal performance for one and two known signals is about 25%. Thus we might not expect a change in the summation index by more than 18-25%. The summation index is defined in RESULTS and DISCUSSION.

4) Is there an effect of peaks-add vs. peaks-subtract phase relations?

Contrast threshold, for the single-channel model which Graham and Nachmias (1971) tested, is determined by the maximum peak-to-trough response in the output image of a single channel. Fig.3.1 shows luminance profiles of the stimuli used in this study. If the filtered images of the $\underline{f}$ and $3\underline{f}$ components have the same

peak-to-trough height at threshold, then the filtered image of the compound grating has 91% greater height for peaks-add phase relation and 63% greater height for peaks-subtract with respect to the peak-to-trough heigth of the 2 c/deg grating. This predicts summation indices of 1.91 and 1.63 for peaks-add and peaks-subtract conditions respectively. In chapter 4, it was found that phase (0^{o} or 180^{o} with respect to the fixation mark) could be recognized as frequently as the signal was detected for a .5 c/deg grating in visual noise but not in the absence of noise. This suggested the possibility that in general the detection of gratings in noise might be mediated by peak detection.

5) Does the psychometric function slope predict the degree of summation?

It will be shown that the psychometric function slopes for detection of the gratings used in this study are significantly shallower for detection in noise than in the absence of noise. Probability summation models (e.g. Quick, 1974; Graham, Robson and Nachmias, 1978) predict that there should be more summation when the psychometric function is shallower.

METHOD

Apparatus

The patterns were produced on the face of a Joyce Electronics CRT display by Z-axis modulation (Campbell and Green, 1965). The display was of the electromagnetic deflection type, with a raster frequency of 100 kHz, and a non-interlaced frame rate of 100 Hz. The display had a P31 phosphor, an unmodulated luminance of 340 cd/m^2, and a dark surround. The viewing distance was 228 cm. The display was 30 cm wide and 16 cm high. Thus, at the viewing distance of 228 cm, the screen subtended 7.5° horizontally by 4° vertically. Photometric calibrations were conducted with an UDT 80X Opto-meter, which was photopic-luminance corrected.

The signal luminance waveforms were synthesized digitally by an LSI-11/23 computer. In each 10 msec frame, the computer generated 300 pairs of voltage samples which were routed through two 12-bit digital-to-analog converters (DAC). One DAC generated the spatial envelope, and the other the sinusoidal grating. The outputs of the two DACs were then multiplied and routed through a programmable dB attenuator which temporally modulated the signal voltage which was subsequently added to the noise.

The luminance noise varied in time and one spatial dimension. Pseudorandom noise was digitally synthesized by a 31-bit shift register with exclusive-or feedback (Roberts, 1963; Horowitz and Hill, 1980; Pelli, 1981). To produce Gaussian one-dimensional noise, the shift register was clocked at f_c and low-pass filtered at the .1 dB downpoint, .1 x f_c. At the maximum rate used (200 kHz), the noise generator would cycle once (2^{31}-1 shifts) in 6 hours.

Stimuli

The luminance at a point x, y (in degrees relative to the fixation mark) at time t (msec) is given by

$$L(x,t) = L_o \times (1 + m(x,t)s(x)),$$

where L_o is the mean luminance. The term $s(x)$ is given by

$$s(x) = c_1\cos(2\pi f_1 x) + c_2\cos(2\pi f_2 x),$$

where c_1 and c_2 are the Michelson contrasts of the 2 and 6 c/deg gratings prior to windowing. Fig. 3.1 shows luminance profiles of the stimuli. The spatial frequencies, f_1 and f_2, were 2 and 6 c/deg respectively. On occasion, the gratings themselves will be referred to as f_1 and f_2. The modulating function $m(x,t)$ is given by the product of Gaussian functions horizontally and temporally

$$m(x,t) = \exp(-(x/s_x)^2-(t/s_t)^2)$$

where s_t and s_x are the time and horizontal space constants respectively. The horizontal space constant was .25°. The time constant was 80 msec. (Note that, because of the Gaussian window,

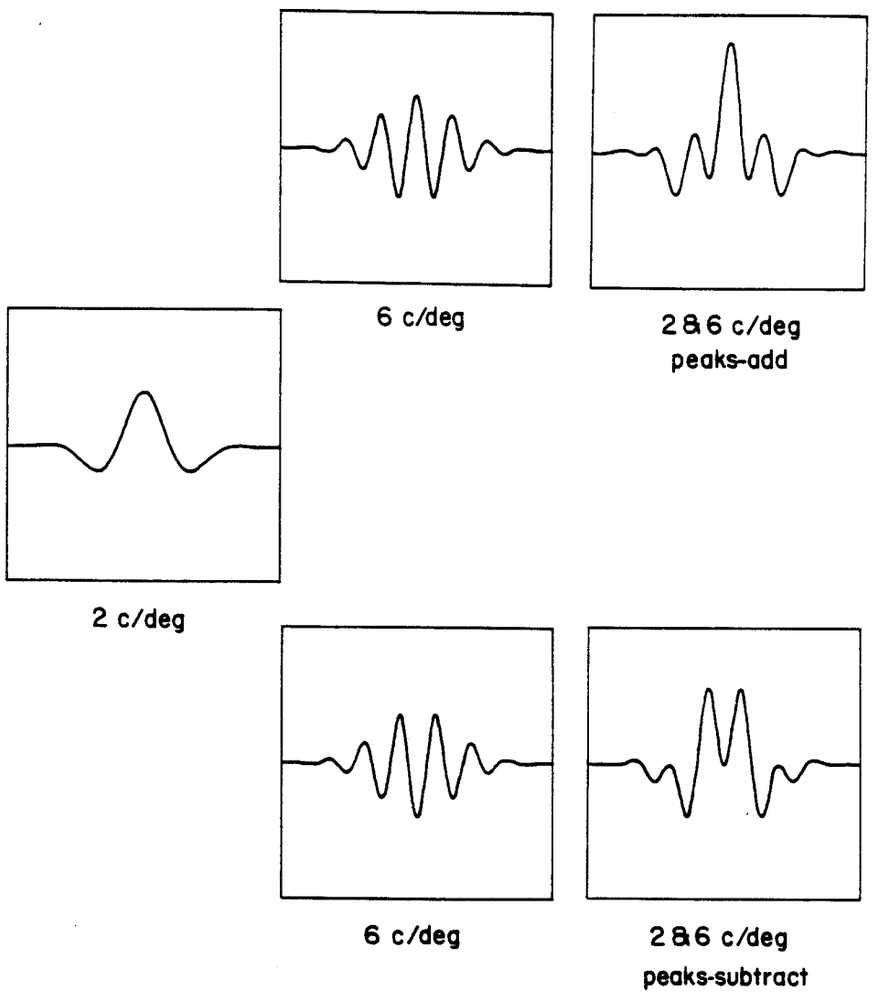

Fig. 3.1. Luminance as a function of visual angle for the 5 stimuli used. The actual contrasts were adjusted so that the 2 and 6 c/deg gratings were equally detectable. The 2 c/deg grating was added to a 6 c/deg grating in either peaks-add (upper panels) or peaks-subtract (lower panels) phase.

the 6 c/deg grating has a peak-to-trough height 29% bigger than the 2 c/deg grating at the same contrast ($\underline{c}_1=\underline{c}_2$).) As measured between 1/e points in the spatial frequency domain, the space constant of .25° confined the horizontal spatial frequency spectrum to 2.2 octaves for the 2 c/deg grating and to .62 octaves for the 6 c/deg grating. Thus the signals were virtually orthogonal, the contrast energy of the cross-term contributing less than 1% of the total contrast energy. Fig. 3.2 shows the spatial frequency amplitude spectra (one-sided) of $\underline{f}_1$ and $\underline{f}_2$ on linear frequency coordinates.

The bandwidth of the noise was always kept flat to 22 c/deg and 50 Hz. The noise spectral density was either 0 or 10^{-5} sec deg. The noise was turned abruptly on 160 msec before the maximum contrast was reached and turned abruptly off 160 msec after the maximum contrast was reached. The noise extended uniformly across the screen and had rectangular spatial and temporal envelopes.

Procedures

Contrast thresholds were measured using a two-alternative forced-choice paradigm. A maximum-likelihood procedure was used to present the signal at the current "best" estimate of threshold contrast (Watson and Pelli, 1983). The contrast yielding 75% correct was estimated. The step size was 1 dB (.05 log units). The intervals were separated by 600 msec. Each interval was marked by an

auditory tone. A feedback tone indicated to the observer whether he was right.

For the psychometric functions, a two-alternative forced-choice procedure was also used. The percent correct was measured in 100 trial blocks for each contrast. There were five blocks at five contrasts per session. To reduce uncertainty, the signal was shown prior to each trial and the same signal was used in all trials in a given block. All psychometric function slopes are based on results from two sessions of 500 or 600 trials each.

For the signal-certain conditions, contrast thresholds were measured in a session consisting of five blocks of 50 trials each. The contrast thresholds for the 2 and 6 c/deg gratings, in cosine-phase with respect to the fixation mark, were measured in blocks 1 and 2 respectively. The stimulus for block 3 was the superposition of the 2 and 6 c/deg gratings in peaks-add phase. The ratio of contrasts was kept constant and was equal to the ratio of the contrasts found in blocks 1 and 2. The contrast threshold for the 6 c/deg grating in anti-cosine phase was measured in block 4. The stimulus for block 5 was the superposition of the 2 and 6 c/deg gratings in peaks-subtract phase, i.e. the superposition of the signals in blocks 1 and 4. The contrast ratio was kept constant in block 5 and was equal to the ratio of the thresholds found in blocks 1 and 4. A disadvantage of this procedure is the possible

introduction of order effects. Possible consequences are discussed later. A sample of the signal was shown 600 msec before the presentation of the first stimulus. The contrast of the sample signal was adjusted to be 30% dB higher in contrast than the current estimate of threshold.

For the signal-uncertain condition, thresholds were measured for the same stimuli as in the signal-certain condition. However, the five signals were randomly interleaved from trial to trial. Sample signals were not shown prior to a pair of trials. Again, 50 trials were used to determine thresholds for each of the 5 stimuli in a session. The contrast ratios of the components in the compound grating were equal to the ratio of the thresholds found in the corresponding signal-certain condition.

The signal-certain and the signal-uncertain conditions were run in the presence or absence of noise. The experimental design enabled measurement of summation for 8 cases: peaks-add or peaks-subtract for signal-certain or -uncertain in the presence or absence of noise. There was a minimum of six sessions for each condition for each observer.

Observers

There were two emmetropic observers, DK and DR. DK was the author. DR was naive to the details of the experiment. Viewing was binocular with natural pupils, and with a fixation point at the center of the screen.

RESULTS and DISCUSSION

Let $\underline{c}^*_1$ and $\underline{c}^*_2$ be the geometric means of the contrast thresholds for the 2 and 6 c/deg gratings when presented alone for a given condition. Let $\underline{c}_1$ and $\underline{c}_2$ be the contrast thresholds of the 2 and 6 c/deg components of the compound grating for a given block of trials. Then the normalized or relative contrasts of the 2 and 6 c/deg components are $\underline{c}_1/\underline{c}^*_1$ and $\underline{c}_2/\underline{c}^*_2$. Figs. 3.3A and B show results for the signal-certain condition in the absence and presence of noise respectively. Figs. 3.4A and B show results for the signal-uncertain case in the absence and presence of noise respectively. The abscissa specifies $\underline{c}_1/\underline{c}^*_1$, the relative contrast of the $\underline{f}_1$ or 2 c/deg component. The ordinate specifies $\underline{c}_2/\underline{c}^*_2$, the relative contrast of the $\underline{f}_2$ or 6 c/deg component. "Ideal" summation is shown by the arc of a circle (see the below for a derivation of this). Each contrast threshold, estimated from a 50 trial block, is shown by a letter of the alphabet. Upper case letters in Figs. 3.3 and 3.4 represent

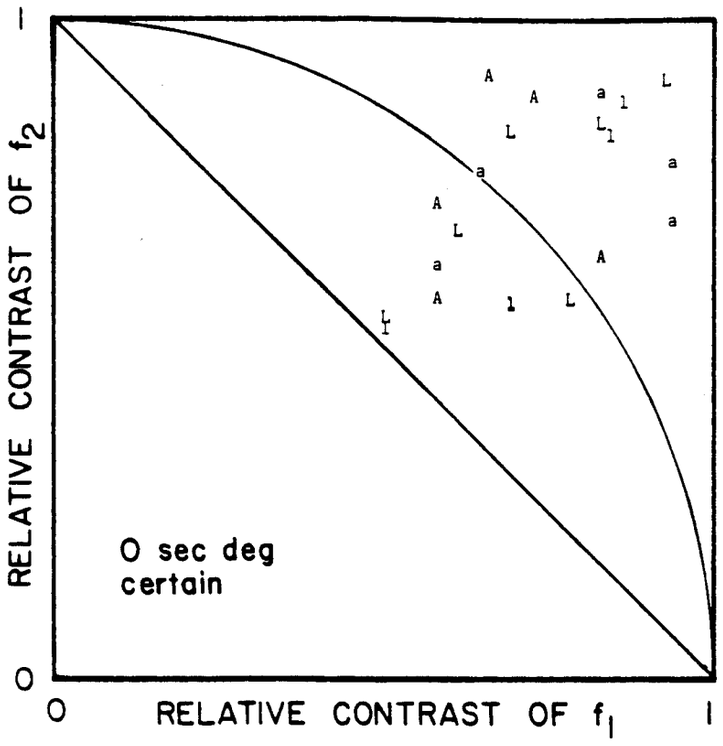

Fig. 3.3A. The relative contrast of the 6 c/deg component (ordinate) vs. the relative contrast of the 2 c/deg component (abscissa) of the compound grating at threshold. "Relative contrast" is the contrast normalized by the contrast threshold of the component grating when presented alone. The circular contour represents "ideal" spatial-frequency summation. The thresholds were measured in the absence of noise. Sample stimuli were shown prior to a trial. The signals were not randomly interleaved. Upper and lower case letters represent data for peaks-add and peaks-subtract phases respectively. A and a represent data for DK, and L and l data for DR.

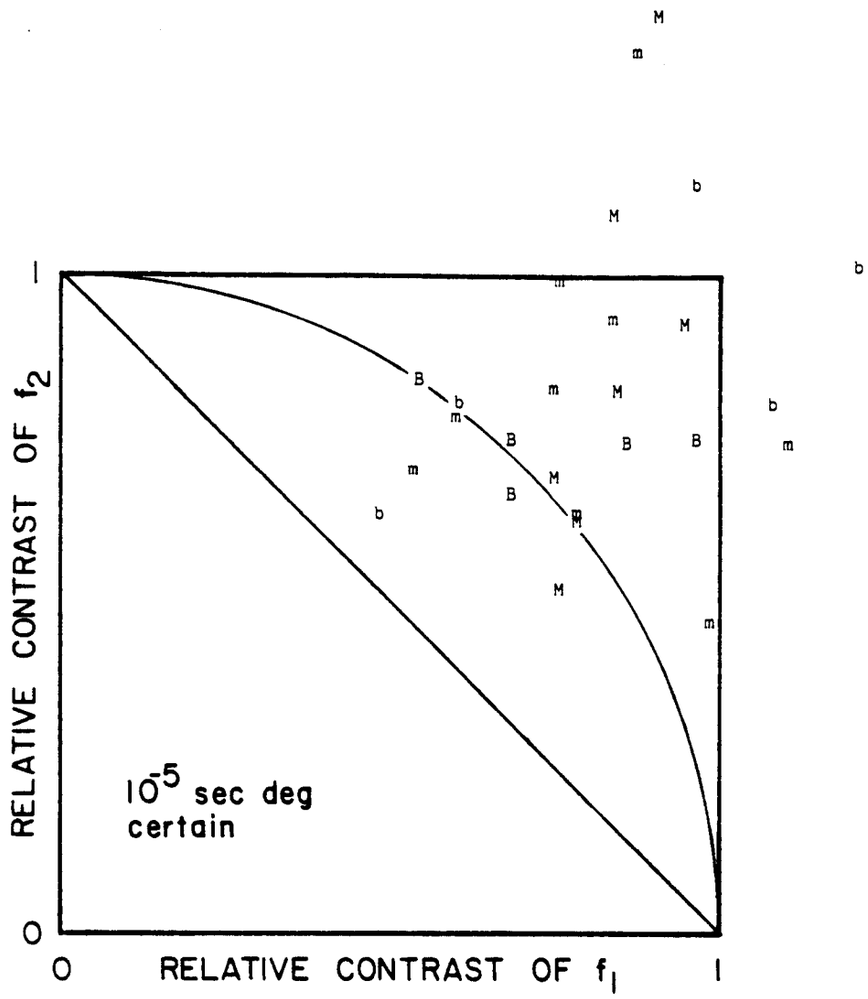

Fig. 3.3B. B and b represent DK's data. M and m represent DR's data. The thresholds were measured in the presence of noise. Other details as for Fig. 3.3A.

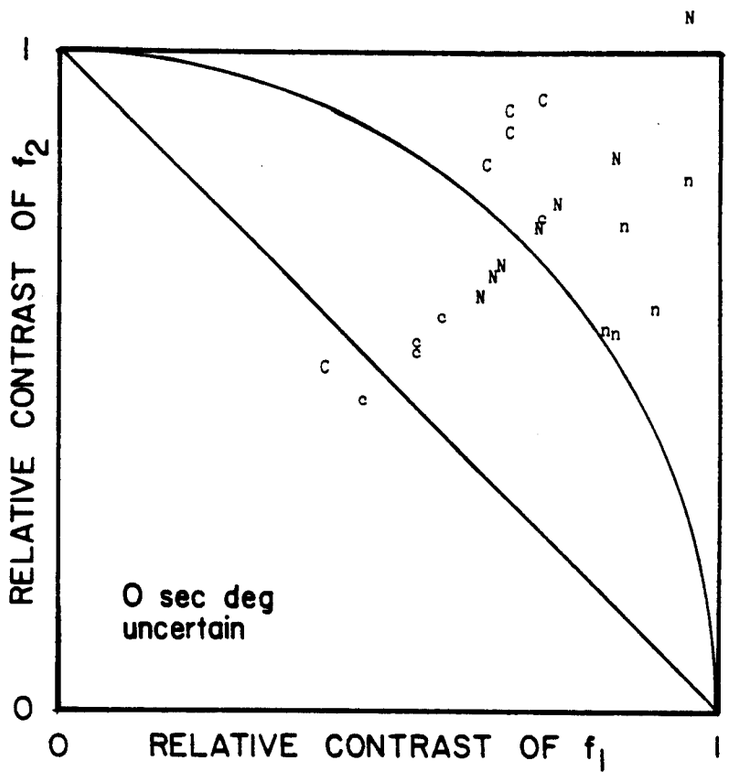

Fig. 3.4A. C and c represent DK's data. N and n represent DR's data. Thresholds were measured in the absence of noise. A sample signal was not shown prior to a trial. The stimuli were randomly interleaved. Other details as for 3.3A.

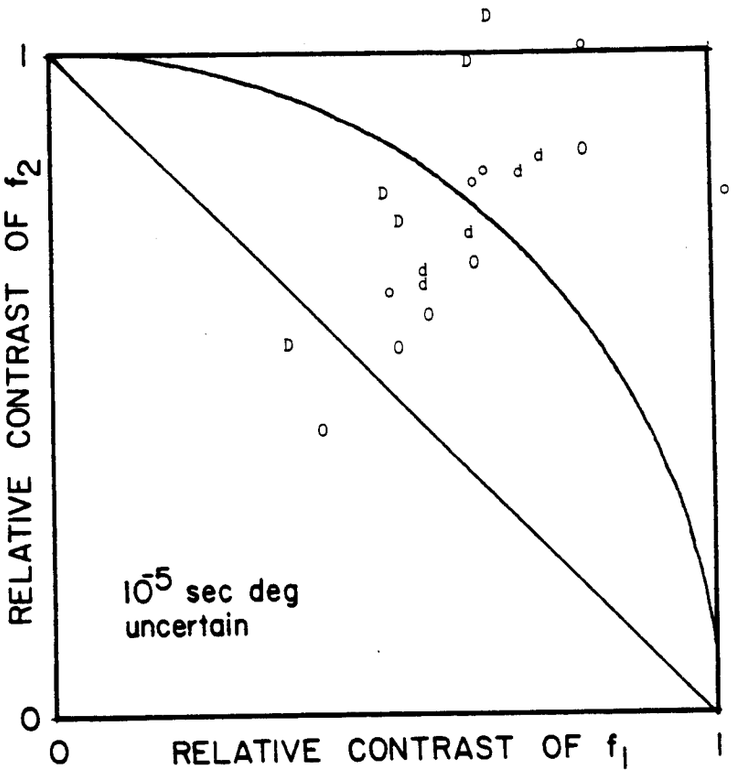

Fig. 3.4B. D and d represent DK's data. O and o represent DR's data. Thresholds were measured in the presence of noise. Other details as for Fig. 3.4A.

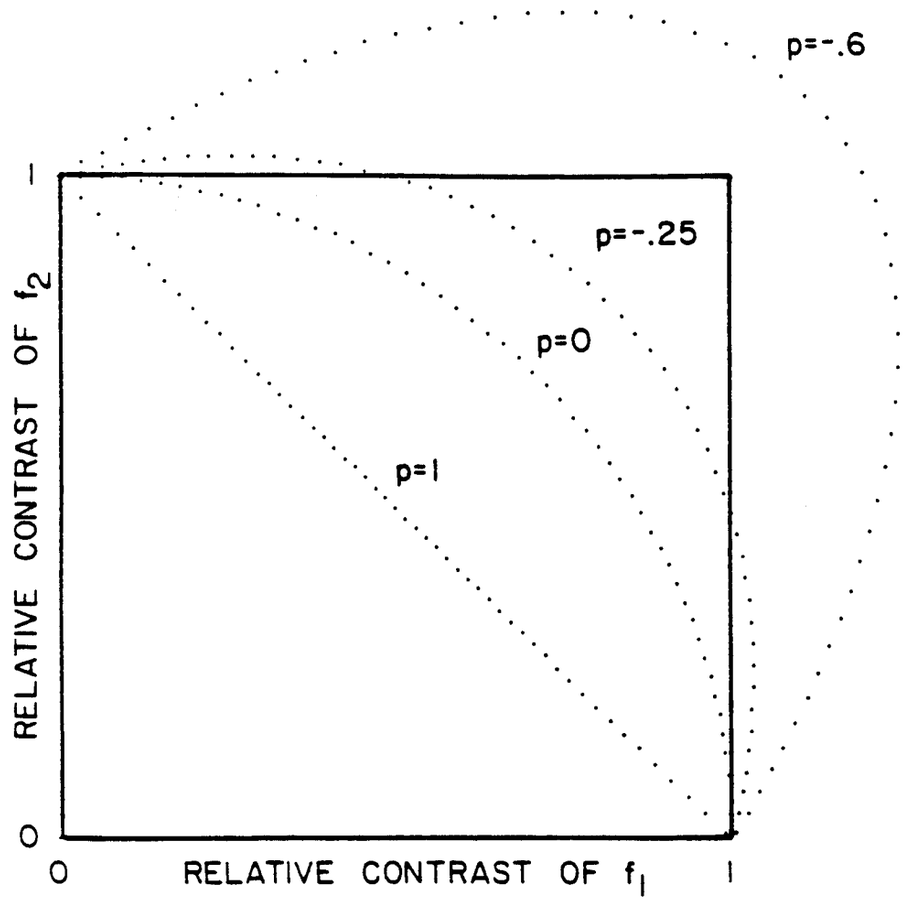

Fig. 3.5. Several contours from the family used to normalize the data from Figs. 3.3 and 3.4. These contours represent ideal spatial-frequency summation for signals with correlations p=1, 0, -.25 and -.6. (The signals used in this chapter had a correlation of 0). Alternatively, these contours represent ideal spatial-frequency summation given correlated noise in two spatial frequency channels with noise correlation coefficients of r (=-p) = -1, 0, .25 and .6.

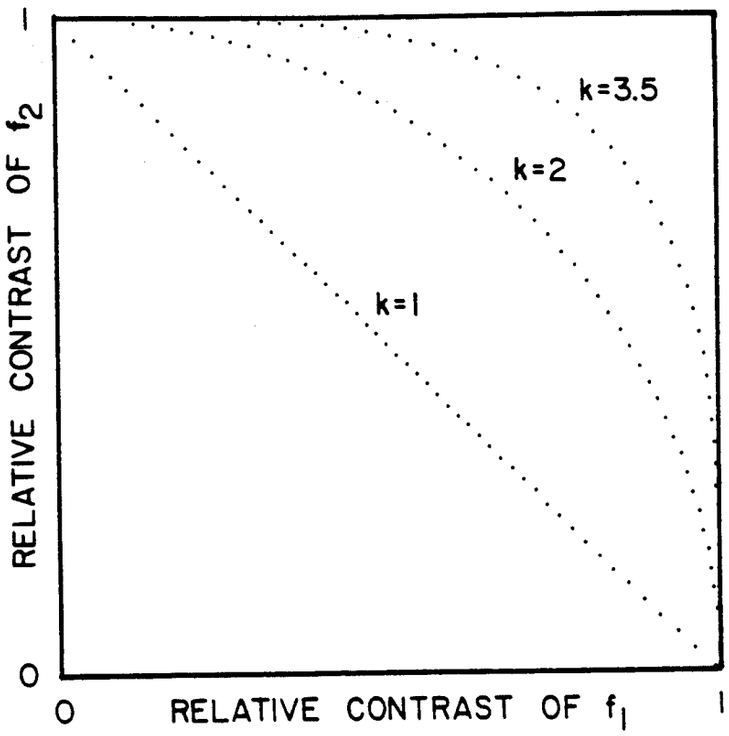

Fig. 3.6. Several contours from the family predicted from probability summation models of spatial-frequency summation.

TABLE 3.1

Three-Way Analysis of Variance
(1/summation index)

Observer : DK

Source of variation	Sum of squares	df	Mean sum of squares	F
Noise	.0555	1	.0555	3.19
Phase	.0061	1	.0061	.352
Certainty	.1343	1	.1343	7.705*
Noise and phase	.0176	1	.0176	1.007
Noise and certainty	.0177	1	.0177	1.016
Phase and certainty	.0681	1	.0681	3.910
Noise, phase and certainty	.0030	1	.0030	.172
Experimental error	.6972	40	.0174	
Total error	.9996	47	.0213	

Arithmetic mean = .729

Observer : DR

Source of variation	Sum of squares	df	Mean sum of squares	F
Noise	.0091	1	.0091	.488
Phase	.0142	1	.0142	.759
Certainty	.0075	1	.0075	.400
Noise and phase	.0093	1	.0093	.499
Noise and certainty	.1408	1	.1408	7.516*
Phase and certainty	.0487	1	.0487	2.601
Noise, phase and certainty	.0308	1	.0308	1.647
Experimental error	.7493	40	.0187	
Total error	1.0098	47	.0215	

Arithmetic mean = .746

* $p < .01$

peaks-add and lower case letters indicate peaks-subtract phase. Letters A - D represent data for DK and letters L - O represent data for DR.

No summation is represented by the upper abscissa and the right ordinate. Summation increases as the origin is approached. Except for Fig. 3.3B, almost all data points are within the unit square. That is, there is non-zero summation for most conditions. Further, except for Fig. 3.3B, most points are scattered close to the ideal-summation contour. Fig.3.3B shows what appears to be significantly less summation for the signal-certain condition in noise. The significance of these observations was assessed using the procedure described below.

Because the estimated ratios of $\underline{c}^*_1$ to $\underline{c}^*_2$ varied slightly from block to block, the points in Figs. 3.3 and 3.4 do not lie along the positive diagonal. A summation index, $\underline{r}_f$, is estimated by the following method, the rationale for which is given below. A parameter $\underline{p}$ defines a contour

$$x^2 + y^2 + 2pxy = 1$$

where $\underline{x}$ and $\underline{y}$ are the abscissa and ordinates of a datum in Fig. 3.3 or 3.4. After solving for $\underline{p}$, we can calculate the value of $\underline{x}$ on the positive diagonal. Call the reciprocal of this value of $\underline{x}$ the summation index ($\underline{r}_f$):

$$r_f = \sqrt{(2 + 2p)}$$

Fig. 3.5 shows contours for various values of p. Ideal summation is defined for p=0 or r_f=1.41, the square root of 2.

Watson (1982) used a family of contours, to derive the summation index defined by

$$x^k + y^k = 1.$$

where $\underline{k}$ uniquely determines a contour (see Fig. 3.6). However, this family of contours does not include points outside the unit square. The reciprocal of the value of x on the positive diagonal is given by

$$r_f = 2^{1/k},$$

which is the summation index based on this family of contours. For points inside the square, Watson's technique gave summation indices equal, within 2%, to those obtained with the method used in the present study.

The three-way analysis of variance (ANOVA) used data from Figs. 3.3 and 3.4 expressed as reciprocals of the summation indices from the relative contrast thresholds. Because some conditions had more data than others for DR, the 6 most recent summation indicies were used to fill each cell of the ANOVA. The three factors were noise level (0 or 10^{-5} sec-deg), the relative phase (peaks-add or peaks-subtract) and the certainty (signal-certain or -uncertain). Table 3.1 shows the results of the linear ANOVA. An ANOVA using the logarithms of the summation indicies was in subtantial agreement. The right-most column contains the F statistic. A single asterisk

indicates $p<.01$. Table 3.2 shows the geometric means of the summation indices for the 8 conditions for DK and DR respectively. With reference to Tables 3.1 and 3.2, we can now return to the questions posed in the introduction.

1) How is spatial-frequency summation affected by noise level?

There are no consistent effects of noise level (apart from the noise-certainty interaction for DR described below) on summation. It seems as though the processes involved in detection at high contrasts in noise are similar to those at low contrasts, in the absence of noise. In one sense, this agrees with the conclusion of Arend and Lange (1980) based on contrast matching. On the other hand, this study shows relatively larger summation closer to that found by Quick, Hamerly and Reichert (1976) using contrast matching. The larger summation showed in the data of the current work would be interpreted by probability summation models as evidence of much broader spatial frequency channels than found before (see below).

2) Is spatial-frequency summation "ideal"?

Consider the ideal detection of two signals which (may or may not be orthogonal) when the signals are exactly specified (Van Trees, 1968). In contrast to the spectra shown in Fig. 3.2, non-orthogonal signals have overlapping spectra. Performance for the ideal detecting a known signal in white Gaussian noise is determined by d'

given by

$$d'^2 = (1/N) \int \{c_1(x) + c_2(x)\}^2 \, dx$$

where $\underline{c}_1(\underline{x})$ and $\underline{c}_2(\underline{x})$ are the contrast functions defined by

$$c_1(x) = c_1 m(x) \cos(2\pi f x).$$

$\underline{N}$ is the noise spectral density (over a two-sided bandwidth), $\underline{c}_1$ and $\underline{c}_2$ are the Michelson contrasts. $\underline{d}'$ is $\sqrt{2}$ times the normal deviate of the proportion correct in a two-alternative forced-choice task. The modulating function is $\underline{m}(\underline{x})$ and has unit peak value. For simplicity only one dimension is considered. The integral of the squared contrast is the contrast energy, denoted by $\underline{E}$. Thus $\underline{d}'$ can be expressed as the sum of two signal-to-noise ratios and a cross-term,

$$d'^2 = (E_1/N) + (E_2/N) + 2p\sqrt{(E_1E_2)}/N, \quad (-1 < p < 1)$$

where $\underline{p}$ is a parameter which indicates the degree of correlation between the two signals. It depends on the relative phase and the spectral overlap of the two signals. If the signals are orthogonal, then $\underline{p}$ is zero. If the two signals are equal, $\underline{p}$ is 1. If one signal is the inversion of the other, then $\underline{p}$ is -1. Contrast energy is proportional to contrast squared. For ideal performance in the experiment in this study, the above equation can be re-written as

$$(c_1/c_1^*)^2 + (c_2/c_2^*)^2 + 2p(c_1/c_1^*)\,(c_2/c_2^*) = 1$$

This follows from the fact that $\underline{d}'^2$ is held constant and is given by

$$d'^2 = \text{constant}_1 \times c_1^{*2} = \text{constant}_2 \times c_2^{*2},$$

for the signal-certain case. This relation is also true for the signal-uncertain case when $\underline{p} = 0$.

TABLE 3.2

Summation index (r_f)

Observer : DK

Phase* (deg)	Noise Spectral Density (sec deg)	r_f** Certain	r_f** Uncertain
0	0	1.45 (1.06)	1.43 (1.09)
180	0	1.32 (1.06)	1.67 (1.09)
0	10^{-5}	1.30 (1.05)	1.47 (1.10)
180	10^{-5}	1.15 (1.12)	1.45 (1.05)
		mean = 1.30	mean = 1.50

Observer : DR

Phase* (deg)	Noise Spectral Density (sec deg)	r_f** Certain	r_f** Uncertain
0	0	1.39 (1.05)	1.32 (1.06)
180	0	1.30 (1.12)	1.24 (1.05)
0	10^{-5}	1.18 (1.08)	1.79 (1.11)
180	10^{-5}	1.24 (1.07)	1.33 (1.08)
		mean = 1.28	mean = 1.40

*For 0°, the second component grating was in cosine-phase relative to the fixation mark, and for 180° the grating was in anti-cosine-phase.

**The geometric means are shown with the corresponding multiplicative standard errors in parentheses.

The summation index r_f is given by

$$r_f^2 = (2+2p).$$

Consider the spectra of gratings f_1 and f_2 as shown in Fig. 3.2. If these two signals are kept in peaks-add phase, as their center frequencies get closer, their spectra begin to overlap, p approaches 1 and the summation index approaches 2. If the signals are in peaks-subtract phase, p approaches -1 as the center frequencies get closer. The summation index approaches zero. Fig. 3.5 shows contours for p = 1, 0, -.25 and -.6, with corresponding summation indices of 2, 1.41, 1.22 and .89. For the signals used in this study, $p \simeq 0$, so the predicted summation index is 1.41. Appendix 3.1 extends the above formulation to ideal combination of information between two channels with correlated noise. This case leads to the same set of contours as above, except that p is replaced by $-r$, where r is the noise correlation in two channels.

For the signal-uncertain case, the results can be summarized by ideal summation. The geometric mean across all signal-uncertain conditions is 1.45. This is not significantly different from 1.41 ($p > .8$, $df=53$ in two-tailed t-test). The geometric mean for the signal-certain case is 1.28. Although somewhat smaller, this is not significantly different from 1.41 ($p > .2$, df=61 in two-tailed t-test). The geometric mean of the summation indices over all conditions and observers is 1.36. Thus, in spite of the small effect of uncertainty (see below), spatial-frequency summation can be well

summarized by ideal-summation.

The assumption of $\underline{d}' \propto \underline{c}$ for the observer may be roughly satisfied for detection in noise (see Table 3.4). However, psychometric function slopes are significantly steeper in the absence of noise. However, this is not critical to the above explanation for the following reason. It is possible that the reason for the steep psychometric function in the absence of noise is due to channel-uncertainty. That is, visual detection can be modeled by an ideal observer which is expecting any one of many orthogonal signals (Pelli, 1981). The performance of a channel-uncertainty model is determined by the contrast energy for a fixed noise level (chapter 4). Because the performance level is constant throughout, the contrast energy threshold is constant for all the conditions. Thus the above derivation remains valid if an arbitrary constant is substituted for $\underline{d}'$ and if $\underline{p} \approx 0$. In fact, whenever performance is determined by contrast energy, one would expect "ideal summation". As pointed out in the INTRODUCTION, channel uncertainty can also be used to account for decreased summation found for increased signal-certainty providing the observer has the ability to switch detection strategy.

It is not often appreciated that the computation of a quantity monotonic with likelihood ratio is easily realized in terms of "receptive field" type elements. Let $\underline{r}(\underline{x})$ be the filtered image (or

"neural image") at the output of a channel representing either noise only or signal (compound grating) plus noise. The likelihood ratio is monotonic with:

$$\int r(x)\{r^*_1(x) + r^*_2(x)\}dx = \int r(x)r^*_1(x)dx + \int r(x)r^*_2(x)dx$$

where $\underline{r}^*_1(\underline{x})$ and $\underline{r}^*_2(\underline{x})$ are the "receptive fields", perhaps at the visual cortex, matched to the expected signals of the neural images, i.e. at the channel outputs. Thus the results of this study can be modeled by a single-channel whose output is $\underline{r}(\underline{x})$ followed by the cross-correlation of the filtered image with the expected signals $\underline{r}^*_1(\underline{x})$ and $\underline{r}^*_2(\underline{x})$. The important point is that "ideal summation" can be realized by a linear detector - the cross-correlator acting on a neural image.

Most previous studies have found summation indices less than 1.41. Only 3 of the more than 50 thresholds plotted by Graham and Nachmias (1971) (see their Fig. 3) had summation indices greater than 1.41. Graham, Robson and Nachmias (1978) and Watson (1982) fit their summation data, for sufficiently different spatial frequencies, with values of $\underline{k}$ between 3 and 4. This corresponds to a summation index between 1.27 and 1.19. Quick, Mullins and Reichert (1978) also find smaller summation indices than 1.41. Graham, Robson and Nachmias (1978) suggest that the greater summation which they found as compared with Graham and Nachmias (1971) is due to greater spatial frequency uncertainty from interleaving the stimuli. The data of this chapter support this explanation. One difference between this

study and previous ones is the narrow width of the window. All of the data collected previously were collected with at least 3 cycles between 1/e points for the lower frequency grating, as compared with 1 cycle in this study. It is not known whether this is a factor in the larger summation found here. As mentioned in the introduction, Limb and Rubenstein (1977) report more summation for reduced fields. Spatial summation tends to reduce estimates of grating summation in probability summation models. Chapter 5 suggests one reason why spatial-frequency summation may be less if the visual system integrates over wide bandwidths and wide fields.

3) Is there an effect of uncertainty on summation or contrast threshold?

Only DK shows a significant effect of uncertainty over all other conditions ($p<.01$). However, there was a significant interaction of noise level and certainty for DR ($p<.01$). This was due to significantly more summation for the signal-uncertain than the signal-certain condition in noise ($p<.01$ in a one-tailed t-test, df=28). There was no reliable effect of certainty in the absence of noise. It can be seen from Table 3.2 that there is more summation for the signal-uncertain than -certain condition. This is in the direction predicted by Graham, Robson and Nachmias (1978). It can also be seen from Table 3.2, that for DR, it is only the data collected in noise which show larger summation for the

signal-uncertain condition.

Table 3.3 shows contrast thresholds for the simple gratings under the various conditions. DK shows greater contrast thresholds for gratings in noise for the signal-uncertain than the signal-certain condition ($p<.025$). DR shows a significant increase in contrast thresholds for both noise and no noise conditions when uncertainty is increased. However, recall that only the noise condition for DR led to a significant increase in summation with signal-uncertainty (see Table 3.2). This would say that in the absence of noise, DR was as uncertain concerning the simple gratings as the compound ones. This null result is in accordance with findings in chapter 4 suggesting greater intrinsic uncertainty for detection in the absence of noise than in the presence of noise. However, this is in conflict with the findings of Graham, Robson and Nachmias (1978) mentioned earlier.

It is possible that the procedure used for the signal-certain case led to order effects. The observer could tire after the first few blocks. Then the estimate of $\underline{c}_1$ would be too high relative to $\underline{c}^*_1$. That is, summation would be under-estimated for the signal-certain case. This would suggest that there is an even smaller effect of degree of uncertainty on spatial-frequency summation than measured. Both observers had more experience with simple gratings from other experiments. This could lead to

spuriously large effects of uncertainty.

4) Is there an effect of peaks-add vs. peaks-subtract phase relations on summation?

Of particular interest is whether a peak-to-trough detector can account for the results, particularly in noise where it has not previously been tested. Recall that the predicted summation indices were 1.91 and 1.63 for the peaks-add and peaks-subtract cases. Summation is much lower than this in noise and in the absence of noise ($p < .05$ for peaks-subtract and $p < .01$ for peaks-add). Further, there is no significant difference in summation index for the two phase conditions (see Table 3.1).

5) Does the psychometric function slope predict the summation index as predicted by probability summation models?

The psychometric function slopes are shown in Table 3.4. The psychometric functions were fit with a maximum likelihood procedure originally developed by Watson (1979) and modifed by Rubin (1982) to fit the data to a straight line defined by

$$\log(d') = m \times \log(\text{contrast}) + \text{constant}$$

where d' is $\sqrt{2}$ times the normal deviate of the proportion correct. The slopes (m) shown in Table 3.2 are the geometric means of the slopes taken from two sessions for each observer. When compared with a pair-wise t-test, both DK and DR show significantly shallower

TABLE 3.3

Contrast Thresholds

Observer : DK

Spatial Frequency (c/deg)	Phase* (deg)	Noise Spectral Density (sec deg)	Contrast** Signal Certain (%)	Uncertain (%)
2	0	0	.76 (1.08)	.85 (1.03)
6	0	0	.75 (1.07)	.64 (1.10)
6	180	0	.69 (1.06)	.75 (1.06)
2	0	10^{-5}	4.97 (1.06)	6.91 (1.06)
6	0	10^{-5}	10.63 (1.05)	9.56 (1.06)
6	180	10^{-5}	9.86 (1.06)	12.03 (1.05)

Observer : DR

Spatial Frequency (c/deg)	Phase (deg)	Noise Spectral Density (sec deg)	Contrast Signal Certain (%)	Uncertain (%)
2	0	0	.64 (1.05)	.69 (1.07)
6	0	0	.68 (1.03)	.70 (1.12)
6	180	0	.55 (1.05)	.72 (1.07)
2	0	10^{-5}	5.73 (1.08)	7.96 (1.08)
6	0	10^{-5}	9.62 (1.06)	12.89 (1.06)
6	180	10^{-5}	12.66 (1.10)	13.92 (1.09)

*For 0°, the second component grating was in cosine-phase relative to the fixation mark, and for 180° the grating was in anti-cosine-phase.

** The contrast thresholds are the geometric means. The standard errors (multiplicative) are indicated by the numbers in parentheses.

TABLE 3.4

Psychometric Function Data

Subject	Spatial Frequency (c/deg)	Width (deg)	Noise Spectral Density (sec deg)	Number of Trials	Slope (m)
DK	2	.25	0	1200	2.31
DK	6	.25	0	1200	3.83
DK	2	.25	10^{-5}	1000	0.91
DK	6	.25	10^{-5}	1000	2.26
DR	2	.25	0	1200	3.09
DR	6	.25	0	1200	2.14
DR	2	.25	10^{-5}	1200	1.25
DR	6	.25	10^{-5}	1200	1.31

slopes for gratings in noise. Probability summation models predict that

$$r_f = 2^{1/k} \approx 2^{.83/m}$$

where k is the slope parameter in the Quick function (Graham, Robson and Nachmias, 1978). A value of m from each session was used to predict a value of r_f for each spatial frequency. A linear one-way analysis of variance was used to compare the predicted values of $1/r_f$ with the measured values pooled over both observers and all conditions. There is no significant difference between predicted values and measured values for the data collected in the absence of noise ($p>.05$). However, for data collected in noise, the measured summation index was smaller than predicted ($p<.01$). It seems that in general, psychometric function slope is not a useful predictor of spatial-frequency summation.

SUMMARY

In summary, the detection of narrowly windowed compound gratings in the presence and absence of visual noise is "ideal-like" in the sense that apart from an attenuation factor, performance is determined by contrast energy.

Appendix 3.1

Correlated noise in two spatial-frequency channels

This appendix describes the optimal way to combine the outputs of two channels which have correlated noise. When this is done, less summation is found than predicted by detection based on contrast energy. Over half of the contrast ratio data plotted by Graham and Nachmias (1971) fall outside of the unit square. The probability summation models of Quick, Mullins and Reichert (1978) and Graham, Robson and Nachmias (1978) only fit points within the square. As mentioned above, the ability to switch detection strategy based on certain or uncertain stimulus conditions may account for points outside the unit square. However, it is worthwhile considering an alternative explanation.

Suppose the outputs of two channels have been reduced to two random variables r_1 and r_2 (e.g. by cross-correlation) with correlation coefficient r. One way in which noise correlation might arise would be if the two channels are non-orthogonal. Then any noise at the inputs to the two channels (e.g. photon or transduction noise) would be correlated. In fact, the noise correlation would increase for broader channel bandwidths with increasing overlap of their pass-bands. It can be shown that the best way to combine the outputs of the two filters is to make use of the fact that the noise

is correlated (Van Trees, 1968, p. 99). The likelihood ratio is monotonic with $\underline{l}$:

$$l = c_1(r_1 - rr_2) + c_2(r_2 - rr_1)$$

Note that $\underline{l}$ could be computed by summing the outputs of two mechanisms which have excitatory inputs from one channel and inhibitory inputs weighted by $\underline{r}$ from the other channel. Ideal performance is given by:

$$d'^2 = \frac{d'^2_1 + d'^2_2 - 2rd'_1d'_2}{(1-r^2)}$$

where $\underline{d}'_1$ and $\underline{d}'_2$ are the performance indices when $\underline{c}_2$ and $\underline{c}_1$ are zero respectively (Van Trees, 1968 p. 99). It is interesting to note that if one of the signals is zero, performance increases to infinity as the noise correlation coefficient approaches -1 or 1. Graham and Nachmias (1971) assumed that if the noises were correlated in two channels, performance would be the same as for one channel. However, this is only true if the observer ignores one of the channels. This throws away useful information which can be used to improve performance. It can be advantagous to "look" with more than one channel even if the signal stimulates only one channel. Consider the example where the correlation coefficient is 1, i.e. the noise in the two channels is perfectly correlated. In this case, the optimal way to make use of this fact is to subtract the output of one channel from the other. If the signal is there, then we are left with only the signal and no noise, if the signal is not there we are left with zero. The ideal makes no errors in this case.

Since the channels are linear, $\underline{d}'^2_1$ and $\underline{d}'^2_2$ are proportional to the squared contrasts of the inputs. The contrast-ratio contours of the can be derived as previously.

$$(c_1/c_1^*)^2 + (c_2/c_2^*)^2 - 2r(c_1/c_1^*)(c_2/c_2^*) = 1$$

The summation index is given by

$$r_f^2 = 2 - 2r$$

Noise signal correlation between two channels is seen to play a converse role to the signal correlation ($\underline{p}$) for the single-channel ideal considered previously. Thus Fig. 3.5 can be interpreted as a family of contours which describe spatial-frequency summation for correlation coefficients (going away from the origin) of -1, 0, .25 and .6.

The data of Graham, Robson and Nachmias (1978) can be fit well assuming a correlation coefficient of .25. The data in this study are fit overall by a correlation coefficient of .06. The above model presumes signal-certainty. However, it is a good approximation for the uncertain case as long as $\underline{r} << 1$.

The possibility of inhibition between spatial frequency channels has been considered by Tolhurst (1972) to explain why there is less adaptation produced by the 3rd harmonic of a square-wave grating than by that component when presented alone. Nachmias, Sansbury, Vassilev and Weber (1973) report similar findings. De Valois (1977) and Tolhurst and Barfield (1978) found that adaptation can result in an

increase in contrast sensitivity to gratings of spatial frequencies far removed from the frequency of the adapting grating. McCourt and Foley (1982) show phase dependent inhibition between spatial frequency components f and $3f$ with the contrast induction effect. Olzack and Thomas (1981) found that frequency discrimination between the components of a compound gratings can be better than detection of the compound grating. They interpreted their results as due to either inhibitory interaction between spatial frequency selective mechanisms or correlated noise or both. There are reports of analogous physiological results. De Valois and Tootell (1982) reported that 97% of simple cells in the cat visual cortex were inhibited by the addition of one or more harmonics. About half of these cells also showed phase dependencies in the amount of inhibition.

REFERENCES

Arend, L.E. & Lange, R.V. (1980). Narrow-band spatial mechanisms in apparent contrast matching. Vision Res., 20, 143-148.

Bergen, J.R., Wilson, H.R. & Cowan, J.D. (1979). Further evidence for four mechanisms mediating vision at threshold: Sensitivities to complex gratings and aperiodic stimuli. J. Opt. Soc. Am., 69, 1580-1587.

Blackwell, H.R. (1963). Neural theories of simple visual discrimination. J. Opt. Soc. Am., 53, 129-160.

Campbell, F.W. & Green, D.G. (1965). Optical and retinal factors affecting visual resolution. J. Physiol., 181, 576-593.

Campbell, R.W. & Robson, J.G. (1968). Application of Fourier analysis to the visibility of gratings. J. Physiol., 197, 551-566.

Cohn, T.E. & Lasley, D.J. (1975). Spatial summation of foveal increments and decrements. Vision Res., 15, 389-399.

De Valois, K.K. (1977). Spatial frequency adaptation can enhance contrast sensitivity. Vision Res., 17, 1057-1065.

De Valois, K.K. & Tootell, R.B. (1982). Spatial frequency inhibition in cat striate cortex cells. Suppl. Invest. Ophthal. & Visual Sci., 22, 206.

Graham, N. & Nachmias, J. (1971). Detection of grating patterns containing two spatial frequencies: A comparision of single-channel and multiple-channel models. Vision Res., 11, 251-259.

Graham, N., Robson, J.G. & Nachmias, J. (1978). Grating summation in fovea and periphery. Vision Res., 18, 815-825.

Graham, N. (1980). Spatial-frequency channels in human vision: Detecting edges without edge detectors. In Visual Coding and Adaptability. C.S. Harris, ed. Hillsdale, N.J., Lawrence Erlbaum Associates.

Green, D.M. (1958). Detection of multiple component signals in noise. J. Acoust. Soc. Am., 30, 904-911.

Horowitz, P. & Hill, W. (1980). The Art of Electronics. Cambridge, Cambridge University Press.

Kelly, D.H. (1961). Visual responses to time dependent stimuli-II. Single channel model of the photopic visual system. J. Opt. Soc. Am., 51, 747-754.

Legge, G.E. (1978). Space domain properties of a spatial frequency channel in human vision. Vision Res., 18, 959-969.

Limb, J.O. & Rubinstein, C.B. (1977) A model of threshold vision incorporating inhomogeneity of the visual field. Vision Res., 17, 571-584.

McCourt, M. E. & Foley, J.M. (1982). Evidence for spatial frequency inhibition in spatial pattern-induction with compound gratings. Suppl. Invest. Ophthal. & Visual Sci., 22, 206.

Mostafavi, H. & Sakrison, D.J. (1976). Structure and properties of a single channel in the human visual system. Vision Res., 16, 957-968.

Nachmias, J., Sansbury, R., Vassilev, A., & Weber, A., (1973). Adaptation to square-wave gratings: In search of the elusive third harmonic. Vision Res., 13, 1335-1342.

Olzack, L.A. & Thomas, J.P. (1981). Gratings: Why frequency discrimination is sometimes better than detection. J. Opt. Soc. Am., 71, 64-74.

Pantle, A. (1973). Visual effects of sinusoidal components of complex gratings: Independent or additive? Vision Res., 13, 2195-2204.

Pelli, D. (1981). Effects of visual noise. Ph.D. Thesis: Cambridge University, England.

Quick, R.F. (1974). A vector-magnitude model of contrast detection. Kybernetik, 16, 65-67.

Quick, R.F., Hamerly, J.R., & Reichert, T.A. (1976). The absence of a measurable "critical band" at low suprathreshold contrasts. Vision Res., 16, 351-355.

Quick, R.F., Mullins, W.W. & Reichert, T.A. (1978). Spatial summation effects on two-component grating thresholds. J. Opt. Soc. Am., 68, 116-121.

Quick, R.F. & Reichert, T.A. (1975). Spatial-frequency selectivity in contrast detection. Vision Res., 15, 637-643.

Ratliff, F. (1965). Mach bands: Quantitative studies on neural networks in the retina. San Francisco, Holden-Day.

Roberts, T.A. (1963). Analysis and synthesis of linear and non-linear shift register generators. Inter. Telemetering Conf., 1, 390-399. IEE, Savoy Place, London.

Robson, J.G. (1980). Neural Images: The physiological basis of spatial vision. In Visual Coding and Adaptability. C.S. Harris, ed. Hillsdale, N.J., Lawrence Erlbaum Associates.

Rubin, G.S. (1982). Suppression and summation in binocular pattern vision. Ph.D. Thesis. Department of Psychology. University of Minnesota.

Sachs, M.B., Nachmias, J., & Robson, J.G. (1971). Spatial-frequency channels in human vision. J. Opt. Soc. Am., 61, 1176-1186.

Schade, O.H. Sr. (1956). Optical and photoelectric analog of the eye. J. Opt. Soc. Am., 46, 721-739.

Tolhurst, D.J. (1972). On the possible existence of edge-detector neurones in the human visual system. Vision Res., 12, 797-804.

Tolhurst, D.J. & Barfield, L.P. (1978). Interactions between spatial frequency channels. Vision Res., 18, 951-958.

Van Trees, H.L. (1968). Detection, Estimation, and Modulation Theory. New York, John Wiley.

Watson, A.B. (1979). Probability summation over time. Vision Res., 19, 515-522.

Watson, A.B. (1982). Summation of grating patches indicates many types of detector at one retinal location. Vision Res., 22, 17-25.

Watson, A.B. & Pelli, D.G. (1983). QUEST: A Bayesian adaptive psychometric method. Percept. & Psychophys., 33, 113-120.

Wilson, H.R. & Bergen, J.R. (1979). A four mechanism model for threshold spatial vision. Vision Res., 19, 19-32.